J. Mar. Biosci. Biotechnol. 2020, p. 29 - 39 Vol. 12, No. 1 [Research Paper]

https://doi.org/10.15433/ksmb.2020.12.1.029 ISSN 2383-5400 (Online)

Carpomitra costata Extract Alleviates Lipopolysaccharide-induced Neuroinflammatory Responses in BV2 Microglia through the Inactivation of NF-κB Associated with the Blockade of the TLR4 Pathway and ROS Generation

Cheol Park[1], Hee-Jae Cha[2], Su-Hyun Hong[3], Suhkmann Kim[4], Heui-Soo Kim[5], Yung Hyun Choi[3*]

[1]Professor, Division of Basic Sciences, College of Liberal Studies, Dong-eui University, Busan 47340, Republic of Korea
[2]Professor, Department of Parasitology and Genetics, Kosin University College of Medicine, Busan 49267, Republic of Korea
[3]Professor, Department of Biochemistry, Dong-eui University College of Korean Medicine, Busan 47227, Republic of Korea
[4]Professor, Department of Chemistry, College of Natural Sciences, Pusan National University, Busan 46241, Republic of Korea
[5]Professor, Department of Biological Sciences, College of Natural Sciences, Pusan National University, Busan 46241, Republic of Korea

(Received 3 May 2020, Revised 11 May 2020, Accepted 11 May 2020)

Abstract In this study, we investigated the inhibitory potential of an ethanol extract of *Carpomitra costata* (EECC) (Stackhouse) Batters, a brown alga, against neuroinflammatory responses in lipopolysaccharide (LPS)-stimulated BV2 microglia. Our results showed that EECC significantly suppressed the LPS-induced secretion of pro-inflammatory mediators, including nitric oxide (NO) and prostaglandin E_2, with no significant cytotoxic effects. EECC also inhibited the LPS-induced expression of their regulatory enzymes, such as inducible NO synthase and cyclooxygenase-2. In addition, EECC downregulated the LPS-induced expression and production of the proinflammatory cytokines, tumor necrosis factor-α and interleukin-1β. In the mechanistic assessment of the antineuroinflammatory effects, EECC was found to inhibit the nuclear translocation and DNA binding of nuclear factor-kappa B (NF-κB) by disrupting the degradation of the κB-α inhibitor in the cytoplasm. Moreover, EECC effectively suppressed the enhanced expression of Toll-like receptor 4 (TLR4) and myeloid differentiation factor 88, as well as the binding of LPS to TLR4 in LPS-treated BV2 cells. Furthermore, EECC markedly reduced the LPS-induced generation of reactive oxygen species (ROS), demonstrating a strong antioxidative effect. Collectively, these results suggest that EECC repressed LPS-mediated inflammatory action in the BV2 microglia through the inactivation of NF-κB signaling by antagonizing TLR4 and/or preventing ROS accumulation. While further studies are needed to fully understand the anti-inflammatory effects associated with the antioxidant activity of EECC, the current findings suggest that EECC has a potential advantage in inhibiting the onset and treatment of neuroinflammatory diseases.

Keywords : *Carpomitra costata*, Anti-inflammation, NF-κB, TLR4, ROS

Introduction

Microglia that act as macrophages in the central nervous system (CNS) play an important role in the development and maintenance of the brain. However, microglia that are hyperactivated in response to inflammatory

* Corresponding author
Phone: +82-51-890-3319 Fax: +82-51-890-3333
E-mail: choiyh@deu.ac.kr

signals damage the brain neurons and cause the onset and progression of various neurodegenerative diseases [10,25]. In particular, pathogenic endotoxins bind to Toll-like receptors (TLRs) and induce excessive activation of microglial cells [1,9]. Among them, lipopolysaccharides (LPS) present in the outer membrane of gram-negative bacteria specifically bind to TLR4. This signal induces the transcriptional activation of the nuclear factor-kappaB (NF-κB) through various intracellular signaling pathways, including phosphatidylinositol 3'-kinase (PI3K)/Akt and mitogen-activated protein kinases (MAPKs), resulting in the expression of a series of inflammatory genes that promote neuronal inflammation and neurodegeneration [16-18]. In addition, microglial cells that are overactivated by LPS induce oxidative stress through increasing the generation of reactive oxygen species (ROS), which further aggravates the inflammatory response [3,14,26]. Therefore, blocking excessive activation of microglia is an important tool to delay the induction and progression of many brain diseases.

Seaweeds have long been used by residents of the Asian coastal regions as sources of medicine and food. Many studies have shown they have various pharmacological effects, including anti-inflammatory and antioxidant effects [4,6,23]. *Carpomitra costata* (Stackhouse) Batters is a kind of brown algae belonging to the Sporochnaceae family. Pesando and Caram [21] found it has both antibacterial and antifungal effects. In addition, *C. costata* has been shown to protect against keratinocyte damage due to ultraviolet B (UVB) rays through an antioxidant mechanism [30]. Recently, it has also been found that the extract of this alga efficiently inhibits the inflammatory response in LPS-treated macrophages [28]. However, studies on microglia have not been performed as of yet; in particular, the role of TLRs in relation to the anti-inflammatory effects of *C. costata* has yet to be clarified. Therefore, this study examined the anti-inflammatory and antioxidant potency of ethanol extract of *C. costata* (EECC) in BV2 microglia stimulated by LPS and investigated the effect of EECC on the activation of TLR4 signaling pathways by LPS.

Materials and Methods

Preparation of EECC

EECC used in this study was provided by the National Marine Biodiversity Institute of Korea (Seocheon, Republic of Korea). For the preparation of the EECC, *C. costata* was collected offshore from Ulleung Island, Republic of Korea, in March 2016. The collected *C. costata* was identified by Dr. Su-Hyun Hong of Dongeui University College of Korean Medicine and washed with tap water to remove the slats, epiphytes, and sands attached to the surface of the samples, and then stored at -20°C. The frozen samples were lyophilized and homogenized, using a grinder before extraction. The dried powder was extracted with 70% ethanol (1:10 w/v) for 1 h (five times) by sonication, and then the extract (EECC) was evaporated in vacuo using a rotary evaporator (Rikakikai Co., Ltd., Tokyo, Japan). The extract was dissolved in dimethylsulfoxide (DMSO, Sigma-Aldrich Chemical Co., St. Louis, MO, USA) before use in the experiment.

Cell culture and treatment

BV2 microglia were maintained in Dulbecco's Modified Eagle's Medium (DMEM), containing 10% (v/v) fetal bovine serum (FBS), L-glutamine (2 mM), penicillin (100 U/ml), and 100 μg/ml streptomycin (100 U/ml, WelGENE Inc., Daegu, Republic of Korea), at 37°C in a humidified atmosphere containing 5% CO_2 and 95% air. To verify the efficacy of EECC in BV2 cells, the medium was exchanged with fresh DMEM, and 100 ng/ml LPS (Sigma-Aldrich Chemical Co.) was added in the presence or absence of EECC for the indicated periods.

Assessment of cell viability

BV2 cells were cultured in 96-well plates at a density of 1×10^4 cells per well. After 24 h incubation, the cells were treated with various concentrations of EECC for

24 h or pretreated with different concentrations of EECC for 1 h prior to LPS (100 ng/ml) treatment for 24 h. Afterward, the medium was removed, 3-(4,5-dimethylthiazol-2-yl)-2,5-diphenyltetrazolium bromide (MTT, 0.5 mg/ml, Sigma-Aldrich Chemical Co.) was added to each well, and they were further incubated at 37°C for 3 h. The supernatant was then replaced with DMSO to dissolve the blue formazan crystals for 10 min. The optical density was measured at a wavelength of 540 nm with an enzyme-linked immunosorbent assay (ELISA) microplate reader (Dynatech Laboratories, Chantilly, VA, USA).

Measurement of pro-inflammatory mediator and cytokine production

The levels of nitric oxide (NO) production were indirectly determined by measuring the stable NO catabolite nitrite in a medium by Griess reaction. To summarize, the conditioned medium was mixed with the same volume of Griess reagent (Sigma-Aldrich Chemical Co.) and incubated for 10 min at room temperature. The optical density at 540 nm was measured with an ELISA microplate reader, and the concentration of nitrite was calculated according to the standard curve generated from known concentrations of sodium nitrite. The levels of prostaglandin E_2 (PGE_2, item No. 500141), tumor necrosis factor (TNF)-α (item No. MTA00B) and interleukin (IL)-1β (item. No. MLB00C) in the culture medium were measured by commercial ELISA kits (Cayman Chemical, Ann Arbor, MI, USA and R&D Systems, Minneapolis, MN, USA) according to the manufacturer's instructions [2].

Protein isolation and Western blot analysis

As described previously [20], the cells were collected and the cellular proteins were prepared. The cytosolic and nuclear proteins were separated using an NE-PER Nuclear and Cytoplasmic Extraction Reagents kit (Pierce Biotechnology, Rockford, IL, USA), according to the manufacturer's protocol. For Western blotting, equal amounts of protein samples were electrophoretically transferred onto polyvinylidene difluoride membranes (Schleicher and Schuell, Keene, NH, USA) following separation in sodium-dodecyl sulfate (SDS) gel electrophoresis. Subsequently, the membranes were blocked with 5% non-fat dry milk/Tris-buffered saline containing 0.1% Triton X-100 (TBST) for 1 h and then probed with specific primary antibodies at 4°C overnight. Antibodies against inducible NO synthase (iNOS, SC-7271, mouse monoclonal), cyclooxygenase-2 (COX-2, SC-19999, mouse monoclonal), IL-1β (SC-7884, rabbit polyclonal), NF-κB (SC-109, rabbit polyclonal), inhibitor of κBα (IκBα, SC-371, rabbit polyclonal), phospho (p)-IκBα (SC-8404, mouse monoclonal), TLR4 (SC-13593, mouse monoclonal), myeloid differentiation factor 88 (Myd88, SC-74532, mouse monoclonal), and β-actin (SC-1615, goat polyclonal) were purchased from Santa Cruz Biotechnology Inc. (Santa Cruz, CA, USA). Antibodies against TNF-α (#37075, rabbit polyclonal) and nucleolin (ab22758, rabbit polyclonal) were obtained from Cell Signaling Technology, Inc. (Danvers, MA, USA) and Abcam, Inc. (Cambridge, UK), respectively. After washing the primary antibodies with TBST, the membranes were incubated with the appropriate horseradish-peroxidase (HRP)-conjugated secondary antibodies (Santa Cruz Biotechnology Inc.) for 2 h at room temperature. The protein bands were detected by an enhanced chemiluminescence (ECL) kit (Amersham Corp., Arlington Heights, IL, USA), according to the manufacturer's instructions.

Electrophoretic mobility assay (EMSA)

EMSA was carried out using the nuclear extracts described in a previous study [13]. To summarize, biotinylation of synthetic complementary NF-κB binding oligonucleotides (Santa Cruz Biotechnology, Inc.) was performed using a biotin 3'-end DNA labeling kit (Pierce Biotechnology) according to the manufacturer's instructions, and annealed at room temperature for 30 min. The mixture was separated by electrophoresis on a 4% polyacrylamide gel that had been pre-electrophoresed in 0.5X Tris-borate buffer for 60 min and then transferred to a nylon membrane (Hybond$^{TM}N^{+}$) for 30

min. Biotin-labeled DNAs were detected using the Light Shift chemiluminescence EMSA kit (Pierce Biotechnology).

Measurement of TLR4 expression on the cell surface

To investigate the effect of EECC on TLR4 expression on the cell surface, Alexa Fluor (AF) 488-conjugated LPS (100 ng/ml, Invitrogen Life Technologies, Carlsbad, CA, USA) was treated with BV2 cells that either were or were not pretreated with EECC for 1 h. After 1 h incubation, the cells were washed twice with phosphate-buffered saline (PBS), harvested with 0.005% ethylenediaminetetraacetic acid (Sigma-Aldrich Chemical Co.), and then analyzed by a flow cytometer. Alexa 488 was excited using 488 argon ion laser lines and detected on channel FL1 using a 530 nm emission filter. Fluorescence emission of the samples was recorded by a flow cytometer (Becton Dickinson, San Jose, CA, USA) as previously described [12].

Detection of the intracellular ROS levels

The production of intracellular ROS was monitored using a cell-permeable fluorogenic probe, 5,6-carboxy-2',7'-dichlorofluorescin diacetate (DCF-DA). To summarize, the cells were treated with EECC for 1 h or pretreated with EECC for 1 h and then cultured for 1 h in either the presence or absence of LPS. The cells were harvested and stained with 10 μM DCF-DA (Sigma-Aldrich Chemical Co.) in the dark at 37°C for 15 min. The cells were then rinsed twice with PBS, and immediately analyzed using a flow cytometer with an excitation wavelength of 480 nm and an emission wavelength of 525 nm. To observe the degree of ROS production by fluorescence microscopic observation, the cells attached to the glass coverslips were stimulated with or without 100 ng/ml LPS after the EECC treatment for 1 h. The cells were stained with DCF-DA, washed twice with PBS, and then fixed with 4% paraformaldehyde (pH 7.4) for 20 min. The fixed cells were analyzed using a fluorescence microscope (Carl Zeiss, Oberkochen, Germany).

Statistical analysis

Data values are expressed as the mean ± the standard deviation (SD). All statistical analyses were performed with GraphPad Prism software 5.0 (GraphPad Software Inc., La Jolla, CA, USA). Comparisons between groups were performed by Dunnett's multiple range tests. Differences were considered statistically significant at $p<0.05$.

Results

Assessment of EECC on cell viability in BV2 microglial cells

To establish the experimental conditions, BV2 cells were treated with a wide range of EECC for 24 h, and cell viability was examined by MTT assay. As shown in Fig. 1A, the cytotoxic effect was not induced at concentrations up to 200 μg/ml, but the cell viability was significantly reduced in the treatment groups with a concentration of 300 μg/ml. In addition, no significant change was found in the EECC concentration up to 200 μg/ml even in the presence of 100 ng/ml LPS (Fig. 1B). Therefore, the maximum concentration of EECC to 200 μg/ml was chosen to study the anti-inflammatory effect of EECC in LPS-stimulated BV2 cells.

Inhibition of LPS-induced NO and PGE2 production by EECC in BV2 microglial cells

To determine the inhibitory properties of EECC on the LPS-induced production of NO and PGE_2, representative pro-inflammatory mediators, BV2 cells were pretreated with different concentrations of EECC for 1 h and then stimulated with or without 100 ng/ml LPS for another 24 h. The levels of NO and PGE_2 in the culture supernatants were determined by Griess reaction assay and ELISA, respectively. As indicated in Figs. 2A and B, stimulation with LPS alone markedly increased NO and PGE_2 production in comparison with no stimulation with LPS. Conversely, EECC significantly inhibited LPS-induced secretion of NO and PGE_2 in BV2 cells in a concentration-dependent manner.

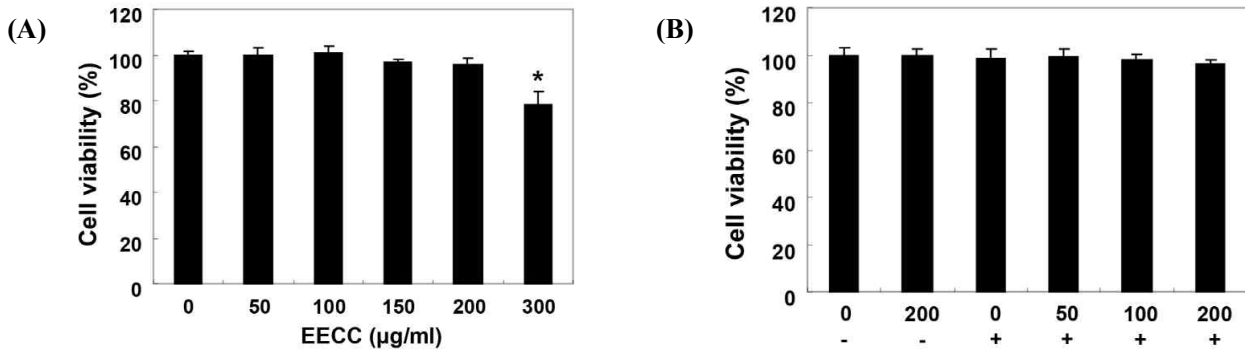

Figure 1. Effects of EECC and LPS on the cell viability of BV2 microglial cells. The cells were treated with various concentrations of EECC for 24 h (A) or pre-treated with the indicated concentrations of EECC for 1 h prior to 100 ng/ml LPS treatment for 24 h (B). The cell viability was assessed with an MTT reduction assay, and the results were expressed as the percentage of surviving cells over control cells. Values represent the means ± SD of the three independent experiments ($^{*}p < 0.05$ compared with the control).

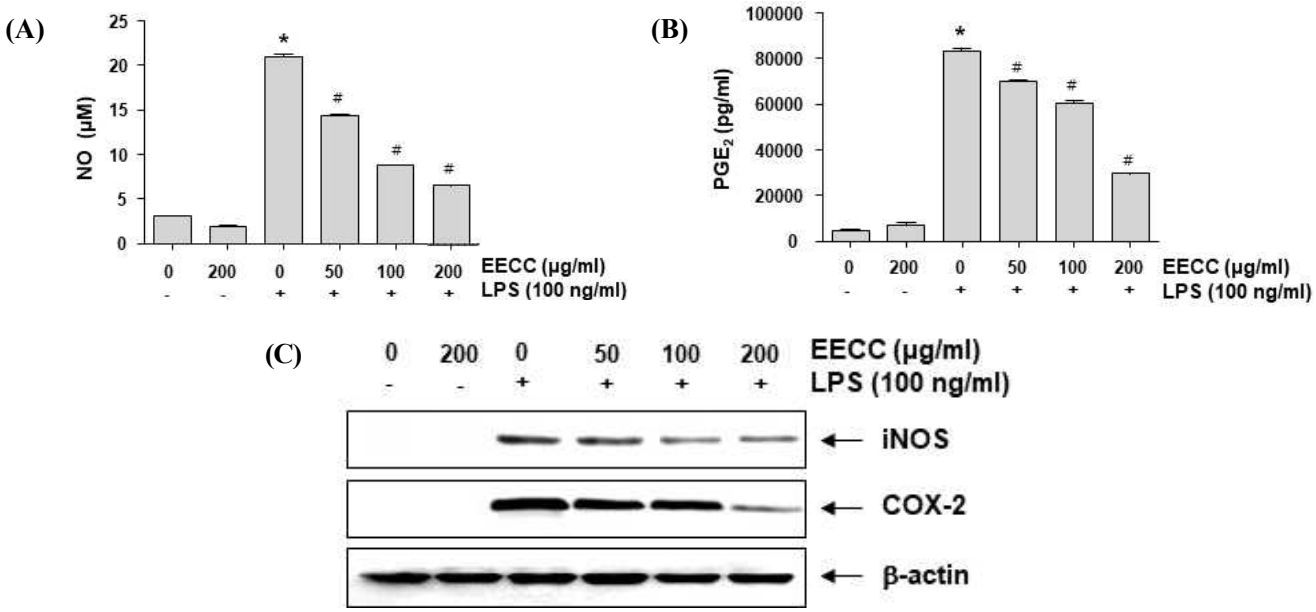

Figure 2. Suppression of NO and PGE_2 production, and iNOS and COX-2 expression by EECC in LPS-stimulated BV2 microglial cells. The cells were pre-treated with the indicated concentrations of EECC for 1 h prior to incubation with 100 ng/ml LPS for 24 h. The levels of NO (A) and PGE_2 (B) in the culture media were measured by Griess assay and an ELISA kit, respectively. Each value indicates the mean ± SD obtained from three independent experiments ($^{*}p < 0.05$ compared with the control; $^{\#}p < 0.05$ compared with the cells cultured with 100 ng/ml LPS). (C) The total proteins were isolated and Western blot analyses were performed using the anti-iNOS and COX-2 antibodies and an ECL detection system. The experiments were repeated three times, and similar results were obtained. β-actin was used as the internal control.

Attenuation of LPS-induced iNOS and COX-2 expression by EECC in BV2 microglial cells

Subsequently, we determined whether the inhibitory effects of EECC on NO and PGE_2 production had to do with regulating the expression of their synthesis enzymes, iNOS and COX-2, respectively. As shown in Fig. 2C, EECC inhibited the expression of the iNOS and COX-2 proteins in the LPS-stimulated BV2 cells. This finding indicates that EECC suppresses NO and PGE_2 production by reducing the expression of their encoding genes.

Reduction of the production and expression of pro-inflammatory cytokines by EECC in LPS-stimulated BV2 microglial cells

The effect of EECC on the production of pro-in-

flammatory cytokines, including TNF-α and IL-6, was next investigated in LPS-stimulated BV2 cells. According to our ELISA results, shown in Figs. 3A and B, the production of these cytokines was significantly increased in the culture medium of LPS-stimulated BV2 cells, which decreased in the presence of EECC in a concentration-dependent manner. In addition, inhibition of TNF-α and IL-6 production by EECC was associated with the suppression of their expressions (Fig. 3C).

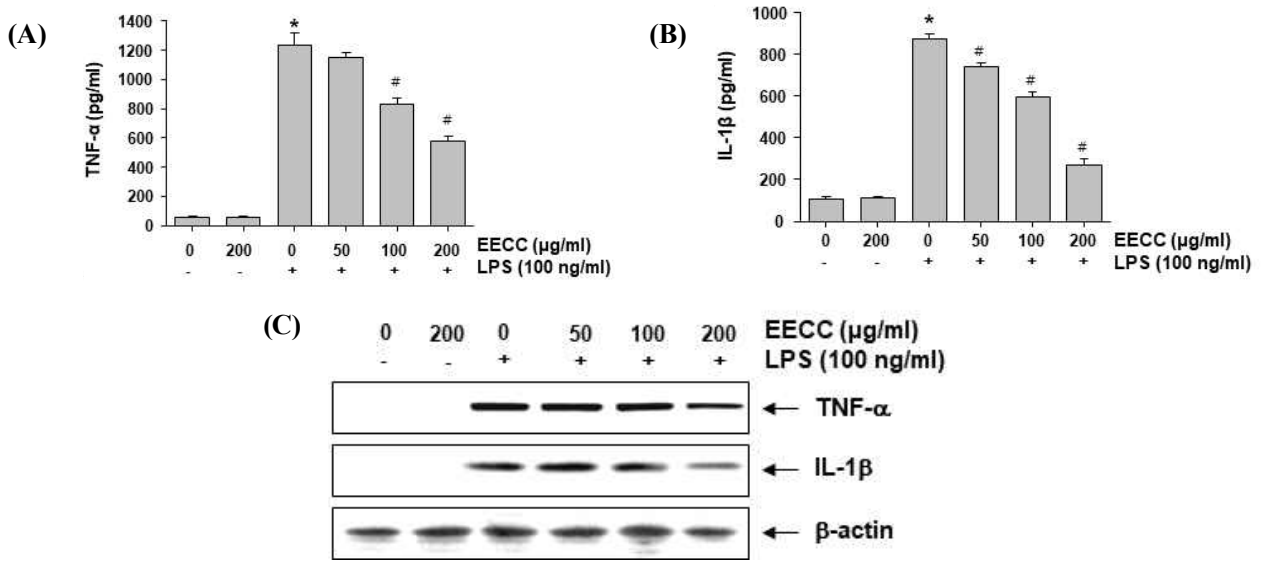

Figure 3. Inhibition of the LPS-induced production and expression of pro-inflammatory cytokines by EECC in BV2 microglial cells. BV2 cells were pre-treated with various concentrations of EECC for 1 h, followed by 100 ng/ml LPS for 24 h. The levels of TNF-α (A) and IL-1β (B) in the culture media were measured by commercial ELISA kits. Each value indicates the mean ± SD obtained from three independent experiments ($^{*}p < 0.05$ compared with the control; $^{\#}p < 0.05$ compared with the cells cultured with 100 ng/ml LPS). (C) The expression of TNF-α and the IL-1β protein was determined using Western blot analyses. β-actin was used as the internal control.

Suppression of LPS-induced activation of NF-κB by EECC in BV2 microglial cells

We next determined whether EECC could attenuate the LPS-induced activation of NF-κB in BV2 cells. Immunoblotting data using cytoplasmic and nuclear extracts showed that EECC pretreatment inhibited the nuclear accumulation of NF-κB p65 subunit associated with the attenuation of IκBα degradation in LPS-stimulated BV2 cells (Fig. 4A). Consistent with these results, the DNA binding activity of NF-κB was markedly increased in the LPS-treated cells, whereas the pretreatment with EECC suppressed the LPS-induced DNA binding activity of NF-κB (Fig. 4B), implying that EECC attenuated the transcriptional activation of NF-κB.

Prevention of LPS-induced TLT4 and Myd88 expressions by EECC in BV2 microglial cells

To determine whether the anti-inflammatory effect of EECC was related to the blocking of the TLR signaling pathway, the effect of LPS and EECC on the expression of TLT4 and Myd88 was investigated. According to the results of immunoblotting (Fig. 5A), the levels of the TLT4 and Myd88 proteins markedly increased in an LPS treatment in a time-dependent manner, similar to the results of previous studies [29]. However, when EECC was pretreated, LPS-induced expression of these proteins was inhibited in a concentration-dependent manner (Fig. 5B), suggesting that EECC may inhibit the LPS-activated TLR4 signaling pathway in BV2 cells.

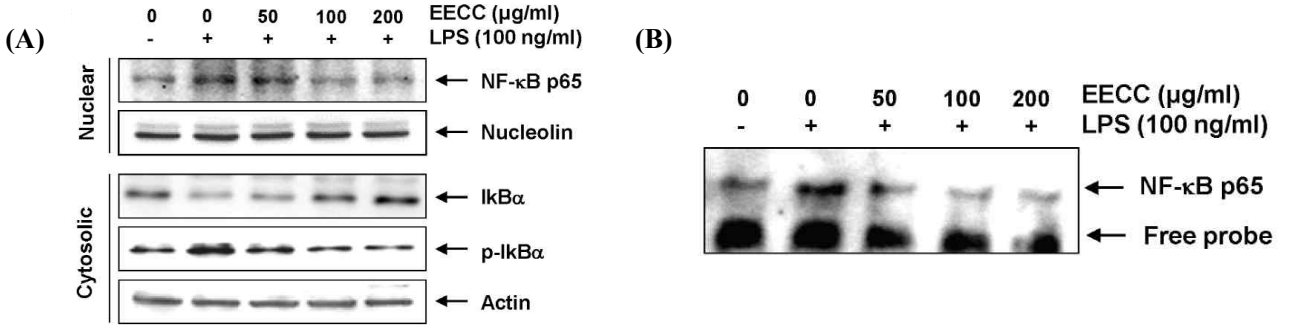

Figure 4. Inhibition of the LPS-induced NF-κB activation by EECC in BV2 microglial cells. (A) The cells were pre-treated with the indicated concentrations of EECC for 1 h before 100 ng/ml LPS treatment for 1 h. The nuclear and cytosolic proteins were prepared for Western blot analysis using anti-NF-κB p65 and anti-IκBα antibodies. Nucleolin and β-actin were used as the internal controls for the nuclear and cytosolic fractions, respectively. (B) Nuclear protein extracts were prepared from the cells cultured under the same conditions and assayed for the DNA binding activity of NF-κB by an EMSA.

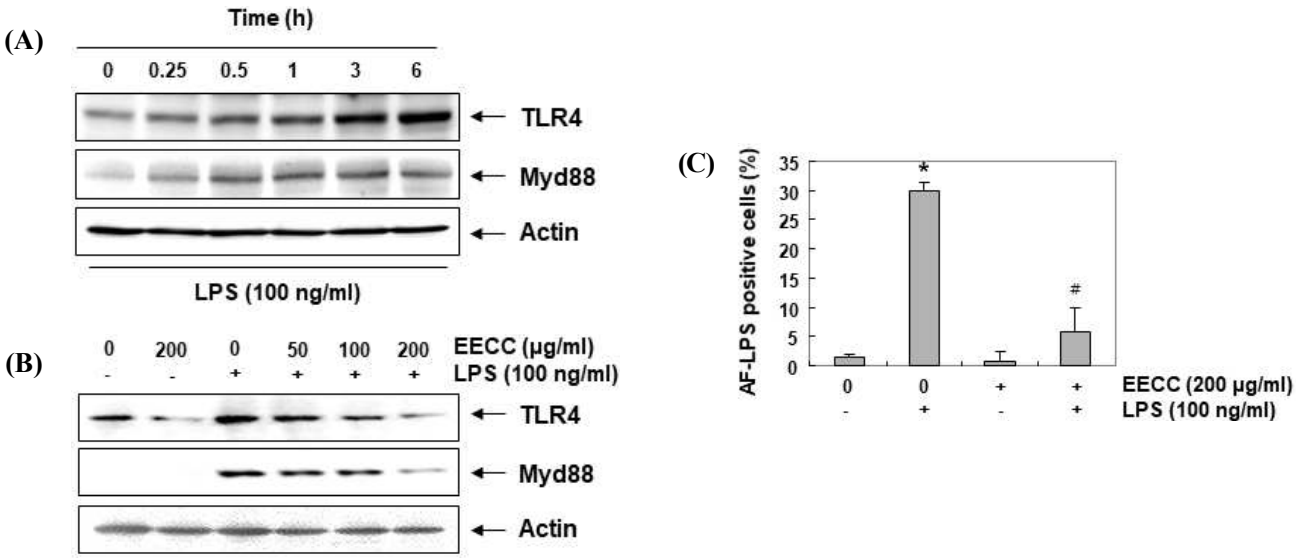

Figure 5. Attenuation of the LPS-induced expression of TLR4 and Myd88, and interaction between LPS and TLR4 by EECC in BV2 microglial cells. The cells were treated with 100 ng/ml LPS for the indicated times (A) or pretreated with the indicated concentrations of EECC for 1 h prior to LPS treatment for 6 h (B). The total proteins were prepared for Western blot analysis using anti-TLR4 and anti-Myd88 antibodies. (C) Following treatment with 100 ng/ml AF-LPS for 30 min in the absence or presence of 200 μg/ml EECC, the LPS binding on the surface of the BV2 cells was measured. Each value indicates the mean ± SD obtained from three independent experiments ($^{*}p < 0.05$ compared with the control; $^{\#}p < 0.05$ compared with the cells cultured with 100 ng/ml LPS).

Suppression of LPS-mediated interaction between LPS and TLR4 by EECC in BV2 microglial cells

We further assessed whether EECC inhibits the interaction between LPS and TLR4 on LPS-treated BV2 cell surfaces. As shown in Fig. 5C, the fluorescence intensity of LPS adhered to the outside of the cell membrane was greatly increased in the cells treated with LPS alone, but significantly attenuated in the cells treated with LPS in the presence of EECC. This indicates that the binding of LPS to TLR4 was suppressed in the presence of EECC.

Protection of LPS-induced ROS generation by EECC in BV2 microglial cells

To investigate the antioxidant potential of EECC, the effect of EECC on LPS-induced ROS production was examined. Our flow cytometry results using the fluorescent probe DCF-DA showed that the level of ROS

gradually increased with the treatment of LPS, peaked at 1 h, and decreased thereafter (data not shown). However, the treatment with EECC alone did not induce ROS generation, and the pretreatment with EECC effectively attenuated the level of ROS released by LPS (Fig. 6A). The inhibitory effect of EECC on ROS production was similarly observed in experiments using fluorescence microscopy (Fig. 6B). In addition, in the N-acetyl cysteine (NAC)-pretreated cells used as a positive control, the production of ROS by LPS was completely blocked, indicating that EECC had a strong ROS scavenging effect.

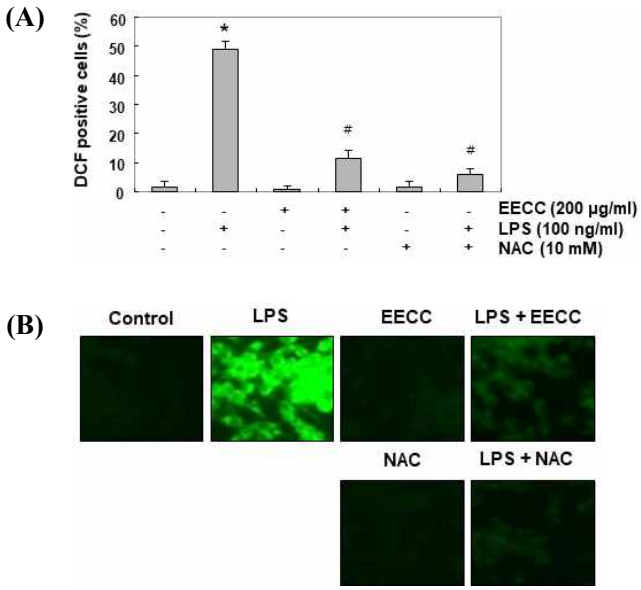

Figure 6. Inhibition of LPS-induced ROS generation by EECC in BV2 microglial cells. Cells were pretreated with 200 μg/ml EECC or 10 mM NAC for 1 h and then stimulated with or without 100 ng/ml LPS for 1 h. (A) The DCF fluorescence was measured by flow cytometry. Each value indicates the mean ± SD obtained from three independent experiments ($^{*}p < 0.05$ compared with the control; $^{\#}p < 0.05$ compared with the cells cultured with 100 ng/ml LPS). (B) After staining with DCF-DA, images were obtained using a fluorescence microscope (original magnification, 200×).

Discussion

Current studies have shown that EECC inhibits LPS-induced inflammatory signaling in a BV2 microglial cell model. Similar to previous studies using a macrophage model [28], our results indicated that EECC significantly inhibited the production of NO and PGE_2 by LPS stimulation in the absence of cytotoxicity, which was associated with the suppression of iNOS and COX-2 expression, respectively. We also found that EECC reduced the release of TNF-α and IL-6 by blocking their expression in LPS-stimulated cells. Therefore, these results suggest that EECC may block the inflammatory response by inhibiting the expression of genes that regulate the production of pro-inflammatory factors.

NF-κB is a key transcription factor that enhances the expression of pro-inflammatory enzymes and cytokines, but only when it has migrated to the nucleus. NF-κB is usually located in the cytoplasm in association with IκBα. When IκBα is phosphorylated and degraded, NF-κB is isolated and translocated to the nucleus [16-18]. Our results indicated that EECC reduced the expression and production of pro-inflammatory mediators and cytokines by inhibiting the NF-κB pathway in LPS-stimulated BV2 microglia. This is also in line with the previous results observed in LPS-stimulated macrophages [28].

Immune cells, including microglia, recognize pathogen-associated molecular patterns through TLRs, pattern recognition receptors expressed on the cell surface. Among the TLRs, TLR4 recruits adapter molecules, including MyD88, an LPS-binding protein and differentiation cluster co-receptor, when activated by LPS [10,25]. Upon activation of TLR4 by LPS, the TLR4–MyD88-mediated signal can induce activation of the intracellular signal transduction systems, including PI3K/Akt and MAPKs. These eventually promote the activation of NF-κB signaling and ultimately produce pro-inflammatory mediators and cytokines [1,9]. In this study, we found that EECC can attenuate the onset of the LPS-mediated intracellular signaling pathway by suppressing the activation of NF-κB and inhibiting the binding of LPS to TLR4 in microglial cells. According to the results of Yim et al. [28], *C. costata* significantly inhibited the LPS-mediated activation of PI3K/Akt and c-Jun N-terminal kinase, but not p38 MAPK and ERK, in the macrophage model. Thus, EECC is expected to

inhibit the NF-κB as well as PI3K/Akt and MAPKs signaling pathways by showing antagonistic effects on the binding of LPS to TLR4 in immune cells such as macrophages and microglia.

Along with inflammatory insults, oxidative stress is another major cause of CNS damage. Low levels of ROS play an important role as signaling molecules to regulate the immune response to pathogens, but overproduction of ROS contributes to neurotoxicity [7,19,26]. In many previous studies, it has been reported that neuroinflammatory response by LPS in microglia was directly related to increased ROS production, and inhibition of inflammatory response was associated with blocking of ROS production [5,8,11,15,22]. Moreover, the TLR4 signaling-mediated generation of ROS by LPS accelerates the inflammatory response by activating downstream signaling cascades containing NF-κB [24,27]; thus, inhibition of ROS production is an important target for suppression of inflammatory responses as well as oxidative stress. Recently, Zheng et al. [30] reported that *C. costata* extract has protective effects against UVB-induced oxidative damage in human keratinocytes involved in blocking ROS production. This antioxidant effect is in line with the current results of EECC, which effectively prevents excessive ROS production. Although the inhibitory effect of EECC on inflammatory response-associated ROS production has been reported for the first time in this study, further studies are needed on the direct link between anti-inflammatory and antioxidant efficacy and the role of intracellular antioxidant systems.

Conclusion

In conclusion, the results obtained in this study demonstrated that EECC had a potent anti-neuroinflammatory effect on BV2 microglial cells. In LPS-stimulated cells, EECC was able to reduce the production of pro-inflammatory mediators and cytokines, which is associated with the decreased expression of their regulatory genes by suppressing NF-κB activity. Furthermore, EECC could block early intracellular signaling cascades by antagonizing against TLR4 or by suppressing ROS accumulation. Although current results may provide a partial understanding of the anti-inflammatory effect of EECC, further studies are needed to assess the major active components of EECC and the mechanical role of EECC in various oxidative stress- and inflammation-mediated diseases.

Acknowledgements

This research was a part of the project titled 'Omics based on fishery disease control technology development and industrialization (20150242)' funded by the Ministry of Oceans and Fisheries, Republic of Korea.

References

1. Cherry, J. D., Olschowka, J. A. and O'Banion, M. K. 2014. Neuroinflammation and M2 microglia: the good, the bad, and the inflamed. *J. Neuroinflammation* **11**, 98.
2. Choi, H. I., Choi, J. P., Seo, J., Kim, B. J., Rho, M., Han, J. K. and Kim, J. G. 2017. *Helicobacter pylori*-derived extracellular vesicles increased in the gastric juices of gastric adenocarcinoma patients and induced inflammation mainly *via* specific targeting of gastric epithelial cells. *Exp. Mol. Med*. **49**, e330.
3. Daulatzai, M. A. 2016. Fundamental role of pan-inflammation and oxidative-nitrosative pathways in neuropathogenesis of Alzheimer's disease in focal cerebral ischemic rats. *Am. J. Neurodegener. Dis*. **5**, 102-130.
4. de Jesus Raposo, M. F., de Morais, A. M. and de Morais, R. M. 2015. Marine polysaccharides from algae with potential biomedical applications. *Mar. Drugs* **13**, 2967-3028.
5. Fan, H., Wu, P. F., Zhang, L., Hu Z. L., Wang, W., Guan, X. L., Luo, H., Ni, M., Yang, J. W., Li, M. X., Chen, J. G. and Wang, F. 2015. Methionine sulfoxide reductase A negatively controls microglia-mediated neuroinflammation *via* inhibiting ROS/MAPKs/NF-κB signaling pathways through a catalytic antioxidant function. *Antioxid. Redox Signal*. **22**, 832-847.
6. Fernando, I. P., Kim, M., Son, K. T., Jeong, Y. and Jeon, Y. J. 2016. Antioxidant activity of marine algal polyphenolic compounds: A mechanistic approach. *J. Med. Food* **19**, 615-628.
7. Fetisova, E., Chernyak, B., Korshunova, G., Muntyan, M. and Skulachev, V. 2017. Mitochondria-targeted antioxidants as a prospective therapeutic strategy for

multiple sclerosis. *Curr. Med. Chem*. **24**, 2086-2114.
8. Garcia, G., Nanni, S., Figueira, I., Ivanov, I., McDougall, G. J., Stewart, D., Ferreira, R. B., Pinto, P., Silva, R. F., Brites, D. and Santos, C. N. 2017. Bioaccessible (poly)phenol metabolites from raspberry protect neural cells from oxidative stress and attenuate microglia activation. *Food Chem*. **215**, 274-283.
9. Glass, C. K., Saijo, K., Winner, B., Marchetto, M. C. and Gage, F. H. 2010. Mechanisms underlying inflammation in neurodegeneration. *Cell* **140**, 918-934.
10. Gomez-Nicola, D. and Perry, V. H. 2015. Microglial dynamics and role in the healthy and diseased brain: a paradigm of functional plasticity. *Neuroscientist* **21**, 169-184.
11. Iizumi, T., Takahashi, S., Mashima, K., Minami, K., Izawa, Y., Abe, T., Hishiki, T., Suematsu, M., Kajimura, M. and Suzuki, N. 2016. A possible role of microglia-derived nitric oxide by lipopolysaccharide in activation of astroglial pentose-phosphate pathway *via* the Keap1/Nrf2 system. *J. Neuroinflammation* **13**, 99.
12. Joh, E. H. and Kim, D. H. 2010. Lancemaside A inhibits lipopolysaccharide-induced inflammation by targeting LPS/TLR4 complex. *J. Cell. Biochem*. **111**, 865-871.
13. Kang, H. J., Jeong, J. S., Park, N. J., Go, G. B., Kim, S. O., Park, C., Kim, B. W., Hong, S. H. and Choi, Y. H. 2017. An ethanol extract of *Aster yomena* (Kitam.) Honda inhibits lipopolysaccharide-induced inflammatory responses in murine RAW 264.7 macrophages. *Biosci. Trends* **11**, 85-94.
14. Kim, S. H., Kim, K. J., Kim, J. H., Kwak, J. H., Song, H., Cho, J. Y., Hwang, D. Y., Kim, K. S. and Jung, Y. S. 2017. Comparision of doxorubicin-induced cardiotoxicity in the ICR mice of different sources. *Lab. Anim. Res*. **33**, 165-170.
15. Kim, Y. E., Hwang, C. J., Lee, H. P., Kim, C. S., Son, D. J., Ham, Y. W., Hellström, M., Han, S. B., Kim, H. S., Park, E. K. and Hong, J. T. 2017. Inhibitory effect of punicalagin on lipopolysaccharide-induced neuroinflammation, oxidative stress and memory impairment *via* inhibition of nuclear factor-kappaB. *Neuropharmacology* **117**, 21-32.
16. Kopitar-Jerala, N. 2015. Innate immune response in brain, NF-Kappa B signaling and cystatins. *Front. Mol. Neurosci*. **8**, 73.
17. Lee, M. B., Lee, J. H., Hong, S. H., You, J. S., Nam, S. T., Kim, H. W., Park, Y. H., Lee, D., Min, K. Y., Park, Y. M., Kim, Y. M., Kim, H. S. and Choi, W. S. 2017. JQ1, a BET inhibitor, controls TLR4-induced IL-10 production in regulatory B cells by BRD4-NF-κB axis. *BMB Rep*. **50**, 640-646.
18. Li, Q. and Verma, I. M. 2002. NF-kappaB regulation in the immune system. *Nat. Rev. Immunol*. **2**, 725-734.
19. Ohl, K., Tenbrock, K. and Kipp, M. 2016. Oxidative stress in multiple sclerosis: Central and peripheral mode of action. *Exp. Neurol*. **277**, 58-67.
20. Park, Y. S., Kwon, Y. J. and Chun, Y. J. 2017. CYP1B1 Activates Wnt/β-catenin signaling through suppression of Herc5-mediated ISGylation for protein degradation on β -catenin in HeLa cells. *Toxicol. Res*. **33**, 211-218.
21. Pesando, D. and Caram, B. 1984. Screening of marine algae from the French mediterranean coast for antibacterial and antifungal activity. *Bot. Mar*. **27**, 381-386.
22. Qin, L., Liu, Y., Hong, J. S. and Crews, F. T. 2013. NADPH oxidase and aging drive microglial activation, oxidative stress, and dopaminergic neurodegeneration following systemic LPS administration. *Glia* **61**, 855-868.
23. Roohinejad, S., Koubaa, M., Barba, F. J., Saljoughian, S., Amid, M. and Greiner, R. 2017. Application of seaweeds to develop new food products with enhanced shelf-life, quality and health-related beneficial properties. *Food Res. Int*. **99**, 1066-1083.
24. Slusarczyk, J., Trojan, E., Glombik, K., Piotrowska, A., Budziszewska, B., Kubera, M., Popiolek-Barczyk, K., Lason, W., Mika, J. and Basta-Kaim, A. 2016. Anti-inflammatory properties of tianeptine on lipopolysaccharide-induced changes in microglial cells involve toll-like receptor-related pathways. *J. Neurochem*. **136**, 958-970.
25. Tremblay, M. È., Stevens, B., Sierra, A., Wake, H., Bessis, A. and Nimmerjahn, A. 2011. The role of microglia in the healthy brain. *J. Neurosci*. **31**, 16064-16069.
26. von Leden, R. E., Yauger, Y. J., Khayrullina, G. and Byrnes, K. R. 2017. Central nervous system injury and nicotinamide adenine dinucleotide phosphate oxidase: Oxidative stress and therapeutic targets. *J. Neurotrauma*. **34**, 755-764.
27. Wang, X., Wang, C., Wang, J., Zhao, S., Zhang, K., Wang, J., Zhang, W., Wu, C. and Yang, J. 2014. Pseudoginsenoside-F11 (PF11) exerts anti-neuroinflammatory effects on LPS-activated microglial cells by inhibiting TLR4-mediated TAK1/IKK/NF-κB, MAPKs and Akt signaling pathways. *Neuropharmacology* **79**, 642-656.
28. Yim, M. J., Lee, J. M., Choi, G., Lee, D. S., Park, W. S., Jung, W. K., Park, S., Seo, S. K., Park, J., Choi, I. W. and Ma, S. Y. 2018. Anti-Inflammatory potential of *Carpomitra costata* ethanolic extracts *via* inhibition of NF-κB and AP-1 activation in LPS-stimulated RAW264.7 macrophages. *Evid. Based Complement. Alternat. Med*. **2018**, 6914514.
29. Yoon, H. M., Jang, K. J., Han, M. S., Jeong, J. W., Kim, G. Y., Lee, J. H. and Choi, Y. H. 2013. *Ganoderma lucidum* ethanol extract inhibits the inflammatory response by suppressing the NF-κB and toll-like receptor

pathways in lipopolysaccharide-stimulated BV2 microglial cells. *Exp. Ther. Med*. **5**, 957-963.
30. Zheng, J., Hewage, S. R., Piao, M. J., Kang, K. A., Han, X., Kang, H. K., Yoo, E. S., Koh, Y. S., Lee, N. H., Ko, C. S., Lee, J. C., Ko, M. H. and Hyun, J. W. 2016. Photoprotective effect of *Carpomitra costata* extract against ultraviolet B-induced oxidative damage in human keratinocytes. *J. Environ. Pathol. Toxicol. Oncol*. **35**, 11-28.